Journal of Drug Targeting

ISSN: (Print) (Online) Journal homepage: https://www.tandfonline.com/loi/idrt20

Improving protection effects of eucalyptol via carboxymethyl chitosan-coated lipid nanoparticles on hyperglycemia-induced vascular endothelial injury in rats

Jianqing Peng , Zhaohui Jiang , Guoping Wu , Zimin Cai , Qianming Du , Ling Tao , Yanyan Zhang , Yi Chen & Xiangchun Shen

To cite this article: Jianqing Peng , Zhaohui Jiang , Guoping Wu , Zimin Cai , Qianming Du , Ling Tao , Yanyan Zhang , Yi Chen & Xiangchun Shen (2020): Improving protection effects of eucalyptol via carboxymethyl chitosan-coated lipid nanoparticles on hyperglycemia-induced vascular endothelial injury in rats, Journal of Drug Targeting, DOI: 10.1080/1061186X.2020.1859514

To link to this article: https://doi.org/10.1080/1061186X.2020.1859514

Accepted author version posted online: 02 Dec 2020.

Journal of Drug Targeting

Original paper

Improving protection effects of eucalyptol via carboxymethyl chitosan-coated lipid nanoparticles on hyperglycemia-induced vascular endothelial injury in rats

Jianqing Peng[a,b], Zhaohui Jiang[a,b], Guoping Wu[a,b], Zimin Cai[a,b], Qianming Du[c,d], Ling Tao[a,b], Yanyan Zhang[a,b], Yi Chen[a,b,*], Xiangchun Shen[a,b,*]

a. The State Key Laboratory of Functions and Applications of Medicinal Plants (The High Efficacy Application of Natural Medicinal Resources Engineering Center of Guizhou Province), School of Pharmaceutical Sciences, Guizhou Medical University, Guiyang 550025, China.

b. The Key Laboratory of Optimal Utilization of Natural Medicine Resources, School of Pharmaceutical Sciences, Guizhou Medical University, Guiyang 550025, China.

c. General Clinical Research Center, Nanjing First Hospital, Nanjing Medical University, Nanjing 210006, China.

d. Department of Clinical Pharmacy, School of Basic Medicine & Clinical Pharmacy, China Pharmaceutical University, Nanjing 210009, China

*Corresponding author

Jianqing Peng, Zhaohui Jiang and Guoping Wu contribute equally to this work.

E-mail address: (Yi Chen) chenyi_19890319@126.com; Tel: +86-0851-88416153

E-mail address: (Xiangchun Shen) shenxiangchun@126.com; Tel: +86-0851-88416151

Abstract

Hyperglycemia is responsible for the major pathophysiological factor of diabetes-associated vascular endothelial injury, which mainly resulted from the disturbance of equilibrium between ROS generation and elimination. Eucalyptol was verified with exact anti-oxidation effects via stimulating the secretion of endogenous antioxidant enzymes against ROS. However, the volatility, instability and poor water solubility of eucalyptol limited its pharmacological activities *in vivo*. In this study, we developed a carboxymethyl chitosan-coated lipid nanoparticles for eucalyptol (CMC/ELN) to facilitate oral administration. A thin lipid film dispersion method was used to prepare the ELN. After CMC coating, the diameter of ELN increased from 166 nm to 177 nm and charge reversal was observed. The nanocarrier enhanced the protective effects of eucalyptol both in the high level of glucose (HG)-damaged HUVECs and endothelial injury in type I diabetes mellitus (T_1DM) rat model. Furthermore, the mechanism of eucalyptol on the promotion of Nrf2 and HO-1 and reduction on Keap1 expression have been verified both in the *in vitro* and *in vivo* model. Besides, the pharmacokinetics data were verified the promotion of the oral eucalyptol absorption by the nanocarrier. Taken together, we established an optimal oral delivery system that promoted oral administration of eucalyptol to exert protective effects on hyperglycemia-induced vascular endothelial injury.

Keywords:

Eucalyptol; endothelial injury; hyperglycemia; lipid nanoparticles; carboxymethyl chitosan

1.Introduction

Hyperglycemia is considered to be a major cause of diabetes-associated vascular disease, which further lead to a series of cardiovascular diseases that are responsible for death worldwide (Sena et al., 2013, Domingueti et al., 2015). Vascular endothelial cells (VECs) are highly specialized and involved in the regulation of thrombosis and inflammation, whereas, the exposure of VECs to high level of glucose (HG) contributed to the endothelial dysfunction (Yang et al., 2020). Accumulating evidence has shown that oxidative stress is the primary cellular event in hyperglycemia-induced vascular endothelium injury. It results in the disturbance of the equilibrium between intracellular reactive oxygen species (ROS) generation and elimination, which leads to irreversible DNA damage, cell senescence and apoptosis (Liu et al., 2020). It was well accepted that surplus of ROS caused disruption of ROS homeostasis is responsible for the dysfunction and death of VECs. Therefore, activation of internal antioxidant system to restore the intracellular ROS homeostasis plays a critical role in protecting vascular endothelium from hyperglycemia-induced injury.

Eucalyptol is a major component of essential oil extracted from aromatic plants (Caldas et al., 2015). It was confirmed that eucalyptol possessed various pharmacological activities, such as an antibacterial (Kifer et al., 2016), a hepatoprotective agent (Murata et al., 2015), an anti-inflammatory (Kim et al., 2015) and an antioxidant (Lima et al., 2013). In our previous studies, eucalyptol has been proved as a strong inhibitor of proinflammatory cytokines via suppression on nuclear factor-kappa B (NF-κB) pathway (Linghu et al., 2016, Linghu et al., 2019). As an antioxidant, eucalyptol was demonstrated to combine with Keap1 and promoted nuclear factor erythroid-2 related factor-2 (Nrf2) expression and translocation from cytoplasm into nuclear (Jiang et al., 2019b). A consequent stimulation of target genes transcription resulted in expression of endogenous antioxidant enzymes, such as NAD(P)H, quinone oxidoreductase 1 (NQO1), hemeoxygense-1 (HO-1), glutamate cysteine ligase (GCL), and glutathione S-transferase A (GSTA), superoxide dismutase (SOD) and catalase (CAT) (Loboda et al., 2016). It is suggested that eucalyptol is a good candidate against ROS surplus via antioxidant and cytoprotective activity.

Oral administration shows great convenience and patient compliance that is preferable for clinical use of eucalyptol. However, the volatility, instability, lipophilicity (log P = 2.74) and low water solubility (3.5 mg/mL) limited the oral medication of eucalyptol due to the low bioavailability and degradation in gastrointestinal tract. Henry's law content (H_c) is the vapor-liquid partition coefficient for the volatile molecules. The H_c value of eucalyptol increased more than ten times from 25 to 60℃ indicating the high volatility (Hammoud et al., 2019). Hence, a propriate formulation of eucalyptol for oral administration are highly in need. Novel drug delivery systems for essential oils have been widely investigated. Nanometric particles have shown great advantages on suppressing volatilization and improving permeation of essential oils through biological barriers (Bilia et al., 2014). Recently, self-microemulsion (Jiang et al., 2019a) and cyclodextrin inclusion compound (Abada et al., 2019) were developed for eucalyptol to facilitate oral administration. Whereas, self-microemulsion without shell outside the emulsion droplet might not prevent the volatilization of eucalyptol and protect it against the gastrointestinal tract environment. The high temperature for certain period of time is inevitable in the preparation of eucalyptol inclusion complex leading to high percentage loss of eucalyptol due to volatilization and degradation. Lipid-based nanocarrier consisted of biodegradable phospholipids with high safety are more favorable for the *in vivo* delivery of essential oils to overcome the physiochemical stability concerns in response to light, heat and other environmental factors. In a previous study, liposomes have been demonstrated to be more attractive for the components from essential oils with extremely low aqueous solubility, the presence of a hydroxyl group and low H_c value (Hammoud et al., 2019). The eucalyptol liposomes prepared in our preliminary experiment showed unsatisfied encapsulation efficiency that might result from the high H_c value and the certain water solubility of eucalyptol. Then, we developed a lipid nanoparticle for eucalyptol that composed of mixed phospholipids, triglycerides and cholesterol esters. It is noteworthy that a preparation method avoiding high temperature heating, high pressure homogenization and long-term solvent evaporation is preferred due to the volatile and thermolabile characteristics of eucalyptol. Therefore, the eucalyptol

loaded lipid nanoparticles (ELN) prepared by a modified thin film dispersion method without heating, homogenization and long-term evaporation was developed in this study to obtain ideal drug loading capacity (LC) and loading rate (LR).

The complex gastrointestinal tract environment followed by oral administration is inevitable and destructive for the drugs. Given that the lipid layer might not strong enough to restrict the leakage and volatilization of eucalyptol, a cover coating on the periphery of ELN might be a promising strategy to avoid destruction in gastrointestinal tract. Meanwhile, effective promotion on transmembrane transportation of ELN across the mucosal barrier is another demand for the functional coating. Chitosan and its derivatives have been widely employed as biocompatible carriers to prevent drugs from degradation in the complex environment of gastrointestinal tract (low pH and various enzymes) (Pyo et al., 2020). What's more, they were capable to enhance the permeation through the intestinal barrier via opening the tight junctions between epithelial cells transiently and remarkable mucosal adhesion (Lopes et al., 2016). These special features make them promising permeation enhancers for efficient oral drug delivery. Carboxymethyl chitosan (CMC) is a hydrophilic derivative of chitosan by carboxymethylation at either C-6 hydroxyl groups or/and the NH_2 moiety as O-CMC, N-CMC and N,O-CMC, which has been widely used as a "shell" of nanoparticles for oral delivery (Upadhyaya et al., 2013). Collectively, CMC was used as the cover for ELN to protect it against gastrointestinal tract environment and promote transportation through intestine mucosa. To guarantee the effective coating of CMC on ELN, N-CMC with high carboxymethylation on NH_2 moiety is preferable to obtain the strong electrostatic attraction between CMC and positive charged ELN.

In this study, we aimed to develop a CMC-coated lipid nanoparticle for the oral delivery of eucalyptol (CMC/ELN) with a modified thin film dispersion method. Absorption promotion effect of the formulations was verified by the pharmacokinetics study using the nile red (NR)-encapsulated LNs. HG-damaged human umbilical vein endothelial cells (HUVECs) were used as *in vitro* endothelial injury model to investigate the protection effects of eucalyptol preparations. *In vivo* evaluation on the

protection effects of eucalyptol preparations was implemented on the type I diabetes mellitus (T_1DM) rat model. Furthermore, the antioxidant mechanism of eucalyptol via regulation on the Nrf2/Keap1/HO-1 signaling pathway was studied both *in vitro* and *in vivo*. Herein, an nanocarrier was developed for eucalyptol to promote the oral absorption and enhance the protection effect on hyperglycemia-induced vascular endothelium injury.

2. Methods

2.1 Materials and reagents

Eucalyptol (purity ≥ 99%, Lot No. H1507047), cholesterol oleate (CO, purity ≥ 85%), glycerol trioleate (GT, purity ≥ 97%) and octadecylamine (ODA, purity ≥ 97%) were supported by Aladdin Reagent Co., Ltd. (Shanghai, China). Soybean lecithin (SPC) was purchased from Lipoid (Ludwigshafen am Rhein, Germany). Polyoxyethylene stearate (SPEG, n = 35~47) and N-CMC (carboxylation degree ≥ 80%) were offered by Macklin Biochemical Co., Ltd. (Shanghai, China). The inorganic chemicals were obtained from J & K Chemical Co., Ltd. (Beijing, China). ODA-fluorescein isothiocyanate (FITC) was prepared according to a previously published report (Yuan et al., 2007). Streptozotocin (STZ, catalogue number: 18883-66-4) was purchased from Sigma (St Louis, MO, USA). Organic solvents of analytical grade were purchased from Aladdin Reagent Co., Ltd. (Shanghai, China).

2.2 Cell culture

Human umbilical vein endothelial cells (HUVECs) and endothelial cell medium (ECM) were purchased from ScienCell Research Laboratories (San Diego, CA, USA). The ECM was composed of basal medium, 5% fetal bovine serum (FBS), 1% penicillin/streptomycin solution (P/S) and 1% endothelial cell growth supplement (ECGS). HUVECs were seeded in poly-L-lysine coated cell culture flasks (NEST, Shanghai, China) at 37℃ with 95% humidity and 5% CO_2. HUVECs were sub-cultured by trypsinization (0.25% trypsin, 0.5 mM EDTA) and three to six passages cells were used in the following experiments.

2.3 Preparation of eucalyptol lodaded LNs

Eucalyptol loaded LN was prepared by a thin lipid film dispersion method.

Briefly, SPC, ODA, CO, GT and SPEG were dissolved in dichloromethane at a mass ratio of 20:1:2:2:1, and then the eucalyptol was added to the mixture at a eucalyptol to SPC mass ratio of 1:3. After vortex for 1 min, we evaporated the solvent at 30℃ using a rotary evaporator (RE52CS, Shanghai Yarong biochemical instrument, Shanghai, China). Then, 4 mL of 0.01M pH 7.4 phosphate buffer (PB) solution was added and incubated with the thin lipid film in a water bath at 25℃ for 1 h. An ultrasonic probe was used to sonicate in the hydration solution at 300 W for 5 min (3 s pulse and 5 s pause) in an ice-water bath. An ultrafiltration tube (molecular weight cut-off, MWCO 100 kDa) was used to remove the unloaded eucalyptol as previously reported (Jiang et al., 2019a). After passing through a 0.45 μm filter, we obtained the eucalyptol lodaded LN (ELN). For CMC coating, a CMC solution dissolved in the 0.01M pH 7.4 PB at concentration of 2 mg/mL was mixed with ELN at a volume ratio of 1:1 and stirred at 500 rpm for 30 min. Optimization on the ratio of SPC to GT, GT to CO and SPC to eucalyptol was studied previously to obtain the optimum prescription.

2.4 Characterization of eucalyptol lodaded LNs

2.4.1 High performance liquid chromatograph (HPLC) analysis of eucalyptol

The concentration of eucalyptol assayed by HPLC/VWD analysis performed with a HP 1260 liquid chromatograph (Agilent Technologies, Palo Alto, CA, USA) with a variable wavelength detector (VWD). Separation was performed on a reversed phase column Welch Ultimate LP-C18 (4.6 × 150 mm, 5 μm, Jiangsu, China), using a mobile phase of acetonitrile and water (56:44, *v*/*v*) at a flow rate of 1 mL/min and detecting at the wavelength of 203 nm. The analysis was performed with oven temperature at 30℃ and the injection volume was 20 μL. A linear regression equation for peak area Y versus eucalyptol concentration was established as Y = 1.5612X - 11.464 (R^2 = 0.9995) at a range of 50 ~ 400 μg/mL. The RSD of precision and reproducibility test was less than 1.5%.

2.4.2 Drug loading rate (LR) and loading capacity (LC)

For the detection of encapsulated eucalyptol, the LNs were 20 times diluted by acetonitrile and sonicated for 20 min to extract eucalyptol. After passing through a 0.45 μm filter, the samples were analyzed by HPLC. The LC and LR of eucalyptol

were calculated according to the following formula (1) and (2).

$$LC(\%) = \frac{W_{drug\ encapsulated}}{W_{total\ LN}} \times 100 \quad (1)$$

$$LR(\%) = \frac{W_{drug\ encapsulated}}{W_{drug\ added}} \times 100 \quad (2)$$

2.4.3 Physiochemical properties and morphology

The particle size, polydispersity and zeta potential of blank LN, ELN and CMC/ELN were measured by Zetasizer (Nano ZS-90, Malvern Instruments, UK). In addition, the morphology of LNs were observed by a transmission electron microscope (TEM, Tecnai 12, Philips, Holland) at an acceleration voltage of 120 kV. LNs were negatively stained with 2% phosphotungstic acid on a copper grid film. Ahead of the observation, the excess liquid was removed by filter paper. *In vitro* drug release behavior of ELN and CMC/ELN was evaluated in 0.1 M HCl (pH 1.2) and 0.01M PB (pH 6.8) by the dialysis diffusion method. Briefly, 1 mL LNs was placed in dialysis bag (MWCO 12 kDa) and immersed in 20 mL of the release medium shaking in an air bath (THZ-82, Beidi Experimental Instrument, Nanjing, China) at 37℃ with 100 rpm. At predetermined time points of 0.5, 1, 2, 4, 6, 9 and 12 h, 200 μL of medium were collected and replaced with fresh medium of equal volume. The amount of eucalyptol was analyzed by HPLC. All release experiments were run in triplicate and conformed with the sink condition.

2.5 In vitro analysis of eucalyptol lodaded LNs

2.5.1 Cellular uptake FITC labeled ELNs

The FITC labeled LNs was prepared with ODA-FITC added at a SPC to ODA-FITC weight ratio of 40:1 in the step of thin film dispersion. Followed by the same preparation procedure in the section "*2.3 Preparation of eucalyptol lodaded LNs*", we received the FITC labeled ELN (FELN) and CMC coated FELN (CMC/FELN). The cellular uptake of FITC labeled LNs was observed by confocal laser scanning microscope (LSM800, Carl Zeiss Meditec AG, Jena, Germany). HUVECs were seeded at a density of 5×10^4 cells/well in a 35 mm glass well and cultured 12 h. After PBS washing twice, we added 2 mL fetal bovine serum (FBS)-free medium containing free ODA-FITC, FITC-ELN, CMC/FITC-ELN at an

equivalent concentration of 0.11 μM FITC for 3 h, respectively. After co-incubation, the HUVECs were rinsed 5 times with ice-cold PBS and fixed by 1 mL of immunostaining fixative for 30 min. Hoechst 33342 was used to stain for 30 min and images of each sample were collected at the excitation wavelength of 350 nm and 488 nm.

2.5.2 Detection of cell viability

HUVECs were seeded in 96 wells plates at a density of 1×10^4 cells/well. HUVECs were incubated with eucalyptol, ELN and CMC/ELN at various concentration for 1.5 h before exposed to the HG environment (35 mM) for 24 h. We removed the medium and added 20 μl of 5 mg/ml MTT. After incubation for 4 h at 37°C, the supernatant was replaced with 150 μL DMSO to dissolve the precipitate. The optical density (OD) of each well was measured at 490 nm using a microplate reader (ELx800; General Electric, Fairfield, CT, USA) with the blank medium as control. The cell viability (%) was calculated according to formula (3).

$$\text{Cell viability (\%)} = \frac{\text{OD}_{\text{sample}} - \text{OD}_{\text{control}}}{\text{OD}_{\text{normal}} - \text{OD}_{\text{control}}} \times 100 \qquad (3)$$

2.5.3 ROS detection

Intracellular ROS accumulation was monitored by staining with fluorescent marker 2,7-dichloroflurescenin diacetate (DCFH-DA) following the protocol. Briefly, HUVECs were cultured with free eucalyptol, ELN and CMC/ELN at equivalent eucalyptol concentration of 0.22 μg/mL and 1.1 μg/mL for 24 h. Then the cells were washed and replenished with DCFH-DA (10 μM) in serum-free culture medium for 30 min at 37°C in dark. Images were grabbed and the fluorescence intensity was measured. The ROS generation was indicated by the fluorescence intensity.

2.5.4 Western blotting

Cells were gathered and then lysed in lysis buffer containing 1 mM phenylmethanesulfonyl fluoride, and the cell lysates were clarified by centrifugation at 12,000 × g for 20 min in 4°C. Protein concentrations in cell supernatants were quantified by a BCA protein assay kit (Beyotime, Institute of Biotechnology, Jiangsu, China). Equal amounts (20 μg) of protein in each group were segregated by 10%

sodium dodecyl sulfate-polyacrylamide gel electrophoresis (SDS-PAGE) and electrotransferred to a polyvinylidene fluoride (PVDF) membranes (Millipore, Bedford, MA, USA). Subsequently, membranes were blocked with 5% bovine serum albumin (Solarbio, Beijing, China) at room temperature for 1.5 h and incubated overnight with Nrf-2/NFE2L2 rabbit polyclonal antibody (Proteintech, Catalog number: 16396-1-AP, 1:1000 dilution), HO-1/HMOX1 rabbit polyclonal antibody (Proteintech, Catalog number: 10701-1-AP, 1:1000 dilution), Keap1 rabbit polyclonal antibody (Proteintech, Catalog number: 10503-2-AP, 1:2000 dilution) and GAPDH mouse monoclonal antibody (Bioworld Technology, Catalog number: AB22431, 1:10000 dilution) at 4°C. After washing, membranes were incubated with secondary antibodies for 1.5 h at room temperature, then visualized with an enhanced chemiluminescence (ECL) kit (7 Sea Biotech, Shanghai, China). Digital images of blots were obtained by a Syngene Gel Imaging System (Bio-Rad, Hercules, CA, USA) and analyzed with Image Lab Software (Bio-Rad, Hercules, CA, USA).

For tissues samples, 50 mg of thoracic aorta tissues was immersed in 200 μL protein lysate (containing 1%PMSF) and homogenized by a glass homogenizer in the ice-water bath. After centrifuged at 12,000 × *g* for 20 min at 4°C, the supernatant protein was quantified by a BCA protein assay kit. Equal amounts (30 μg/10 μL) of protein in each group were segregated by 10% SDS-PAGE and electrotransferred to a PVDF membranes (Millipore, Bedford, MA, USA). The following processing procedure is the same with cell samples.

2.6 Pharmacokinetic studies of NR-encapsulated ELNs

Male Sprague-Dawley (SD) rats (180–200 g) supplied by Guizhou Medical University Laboratory Animal Co., Ltd. (Guiyang, China) were housed under controlled temperature (22 ± 3℃), humidity (50 ± 20%) with standard laboratory food and water. The following animal studies strictly complied with protocols approved by the Animal Welfare and Ethics Committee (AWEC, Guizhou Medical University, NO. 1900147), and all procedures were in accordance with the National Institute of Heath's guidelines regarding the principles of animal care.

To evaluate the absorption promotion effect of ELNs, the NR-encapsulated ELNs

was prepared. The NR dissolved dichloromethane was added in the step of thin film dispersion. Followed by the preparation procedure in the section "*2.3 Preparation of eucalyptol lodaded LNs*", we received the NR-encapsulated ELNs (NELN) and CMC-coated NELN (CMC/NELN). Male SD rats were randomized into three groups (n = 6) and oral administrated with free NR, NELN and CMC/NELN at an equivalent dose of 1.5 mg/kg NR, respectively. Blood samples were taken via femoral vein at 0.25, 0.5, 1, 2 4, 6, 8, 12 and 24 h and centrifuged at 1,500 × *g* for 10 min at 4°C. Two-hundred μL of plasma was mixed with 800 μL acetonitrile and vortexed 1 min for NR extraction. The mixture was centrifuged at 10,000 × *g* for 15 min at 4°C and 500 μL of supernatant was analyzed at Ex/Em of 530/635 nm via a Varioskan LUX reader (Thermo Scientific, Vantaa, Finland). The plasma concentrations of NR were analyzed by Win Nonlin 5.2.1 (Pharsight, Mountain View, CA, USA).

2.7 T_1DM mice model establishment and treatments

2.7.1 T_1DM mice model establishment

T_1DM rat model was established via intraperitoneal injection of streptozotocin at 50 mg/kg in sodium citrate buffer (0.05 M, pH 4.5). The fasting blood glucose (FBG) level of rats was detected 3 days after injection and the successful establishment of T_1DM rat model was diagnosed once the FBG level higher than 16.8 mM for two consecutive days. Then, the model rats were randomly divided into four groups (n = 6): Model, Eucalyptol, ELN and CMC/ELN at an equivalent eucalyptol dose of 18 mg/kg. Eucalyptol solution was solubilized in PBS (0.01 M, pH 7.4) containing 2% Tween 80 at concentration of 3.5 mg/mL. Normal SD rats were used as control. Both control and model groups were treated by the same volume of PBS (0.01M, pH 7.4). The preparations were orally administered every other day for one month. At the end of study, blood samples were collected and centrifuged at 1500 × *g* for 10 min at 4℃. The supernatant was collected for ELISA assay. All rats were sacrificed to dissect thoracic aortas (about 0.5 cm in length fixed in 10% neutral buffered formalin) and stored at -80℃.

2.7.2 Hematoxylin-Eosin (H&E) Staining

Thoracic aorta tissues were fixed in 10% formalin and embedded in paraffin.

After 5 μm sections prepared, the samples were applied with H&E staining for the observation of lesions and abnormality of vessels under an optical microscope (Leica DMi8, Germany) with photo-micrographic attachment at 100 × magnification.

2.7.3 Enzyme-Linked Immunosorbent Assay (ELISA)

Protein levels of IL-6, TNF-β and IL-1b in serum of T_1DM rat after treatment were determined using an ELISA kit (MEIMIAN, Yancheng, Jiangsu, China). The absorbance was detected by a microplate reader (ELx800; General Electric) at 450 nm.

2.7.4 Immunofluorescence

Immunofluorescence staining of paraffin sections was blocked in 2% bovine serum albumin (BSA) for 1 h and incubated overnight with anti-Nrf2 antibody (1:100 dilution), anti-HO-1 antibody (1:100 dilution) and anti-Keap1 antibody (1:100 dilution) at 4℃. Then the samples were rinsed in PBS and incubated with biotinylated secondary antibody for 30 min followed by peroxidase-conjugated streptavidin for 30 min. After counterstained with hematoxylin, images of each sample were captured by using a confocal microscope (ZEISS, LSM710) (nuclei with DAPI staining, blue; Nrf2 with Cy3 staining, red; HO-1 with Cy5 staining, purple; Keap1 with FITC staining, green). Image J (National Institutes of Health, USA) was used to analyze fluorescence intensity of each sample, and GraphPad Prism7.0 was used for statistics and graphing.

2.8 Statistical analysis

The data are processed using GraphPad Prism 5 (La Jolla, CA) and presented as mean ± standard deviations (S.D.) of at least three independent experiments. Statistical significance was determined using the independent-samples *t* test between control and model groups and one-way ANOVA followed by post-hoc Tukey test among model and treatment groups. The *p* value of less than 0.05 was statistically significant.

3. Results and discussion

3.1 Preparation and optimization of eucalyptol-loaded LN

In our previous studies, high dose of eucalyptol (50-300 mg/kg) is orally administrated as suspension (Linghu et al., 2019) or self-microemulsion (Jiang et al.,

2019a) for the alleviation of endothelium injury induced by the lipopolysaccharide, despite the low effective dose *in vitro*. We believe that the low delivery efficiency *in vivo* might be the main reason for the high oral dose. The suspension particles and emulsion droplets that successfully maintained the eucalyptol in the aqueous solution might not strong enough to prevent the volatilization and promote the absorption of eucalyptol after oral administration. Therefore, a more effective delivery system for oral administration of eucalyptol is highly in need. Based on the previous study, eucalyptol exerted extremely low LR in the encapsulation by liposomes via ethanol injection method (Hammoud et al., 2019). The thin film dispersion method used for the preparation of liposomes in our preliminary experiment obtained similar LR of eucalyptol as well (data not shown). It is attributed to the high H_c value that impedes the encapsulation of eucalyptol in the hydrophilic core of liposomes. Therefore, LNs with lipophilic core were applied for the encapsulation of eucalyptol in this study, which was expected to stabilize the eucalyptol inside the lipophilic core of nanoparticles and reduce the volatilization.

The weight ratio of SPC:GT, GT:CO and SPC:eucalyptol were optimized in the preparation of ELN in terms of LR and LC of eucalyptol (**Figure S1**). GT promoted the LR and LC of eucalyptol and exerted an optimum value at SPC/GT weight ratio of 10:1. It is suggested that the presence of the lipophilic core inside LN provided by GT contributes to the improved encapsulation of eucalyptol within certain range. For the weight ratio of GT/CO, the LC and LR were similar at 2:1 and 1:1. Since high ratio of GT made no contribution to the encapsulation of eucalyptol, GT/CO weight ratio of 1:1 is preferable. It was noteworthy that the LR increased along with the weight ratio of SPC:eucalyptol and reached approximately 80% at 3:1, while LC showed no significant difference. Thus, the encapsulation of eucalyptol is in direct proportion to the amount of SPC, which indicated that abundant lipids is the key factor for the encapsulation of eucalyptol. The final weight ratio of SPC:CO:GT:eucalyptol at 30:3:3:10 was used.

In the preparation of ELN, the temperature is a key factor that profoundly affects the loss of eucalyptol. According to the H_c value, gaseous phase of eucalyptol

increases tenfold as the temperature rises from 25 to 50°C (Hammoud et al., 2019). Given that both the high temperature and strong sonication led to the evaporation of eucalyptol, the step of lipid film formation and hydration in the preparation were carried out below 30°C and sonicated at a power of 300 W by an ultrasonic probe for 5 min. Due to the roles of hydration and sonication played in the reduction and uniformization of particles size, we have to make a compromise between the satisfied diameter/PDI of ELN and expectable LC/LR of eucalyptol.

A CMC layer is capable to form protective shell outside the ELN through electrostatic adsorption to facilitate the oral delivery of eucalyptol. SPEG was inserted on the surface of ELN possessing sufficient steric hinderance to prevent the intense interactions between CMC and ELN that might lead to aggregation. In addition, PEG chains could improve the stability of ELN in the circulation after passing through the gastrointestinal mucosa. The LC and LR of eucalyptol in the final optimized ELN and CMC/ELN were detected (**Table 1**) and CMC-coating slightly reduced the encapsulation of eucalyptol. It might be attributed to the dissociation of the adsorbed eucalyptol on the surface of ELN due to the interference from coated CMC.

3.2 Characteristics of blank LN and eucalyptol-loaded LNs

The schematic structure of CMC/ELN indicated the role of each component played in the nanoparticles (**Figure 1A**). Both blank LN and CMC/ELN was observed under TEM (**Figure 1B, C**). Small size, single layer and internal cavity were clearly shown in the image of blank LN. However, larger particles with multilayer and fluffy edge was observed in the image of CMC/ELN, which indicated the successful encapsulation of eucalyptol and coating of CMC. In corresponding to the morphological observation, the measurement of diameter, PDI and zeta potential by a Zetasizer (**Table1**) manifested that the diameter of LN increased 50 nm after eucalyptol loaded, while PDI decreased to less than 0.25 (**Figure 1D**). It is suggested that the eucalyptol fills the lipophilic core of LN and reconstructs the nanoparticles resulting in improved uniformity of particle size. Although CMC-coating did not increase the diameter and PDI of ELN, a charge reversal was detected indicating the successful preparation of CMC/ELN (**Figure 1E**).

In vitro release profiles of eucalyptol from ELN and CMC/ELN in pH 1.2 and pH 6.8 medium are shown in **Figure 1F.** More than 70% of eucalyptol loaded was maintained after 12 h in both ELN and CMC/ELN, which indicated the sufficient protection on eucalyptol in the gastrointestinal tract after encapsulation. However, similar release curves were observed for ELN and CMC/ELN at pH 1.2. Although the release rate of eucalyptol from CMC/ELN was retarded at initial 4 h in pH 6.8 medium, the cumulative release after 9 h is the same with that of ELN. The results indicate that CMC-coating is not strong enough to further prevent the leakage and volatilization of eucalyptol against the gastric and intestinal juice that closely related to the weakened interactions between CMC and ELN over time.

3.3 Evaluation of FELN and CMC/FELN uptake by HUVECs

Intracellular distribution of ELN was observed by the confocal microscopy after FITC labeling (**Figure 2A**). Free FITC showed slight cellular uptake resulting from the simple diffusion of small molecules. FELN exhibited remarkable uptake in HUVECs after 3 h incubation. The positive surface potential might contribute to the cell adhesion and uptake, which was further verified by the significant reduction on the intracellular fluorescence of CMC/FELN that possessed negative surface potential. Although the CMC-coating interfered the cellular uptake of eucalyptol by HUVECs, it will not significantly affect the activity of eucalyptol in endothelial cells *in vivo* as the CMC might remained in the apical side when crossed through the mucus layer (Tang et al., 2018). Besides, the interactions between CMC and ELN weakened over time in the gastrointestinal tract and circulation contributed to the disassociation before the cellular uptake of endothelial cells *in vivo*.

3.4 Protective effect of eucalyptol preparations on the HG-damaged HUVECs

To evaluate the protective effect of eucalyptol preparations and blank carriers, an HG-damaged HUVECs model was established, which exhibited more than 20% reduction on the cell viability. Both of ELN and CMC/ELN showed obvious protective effect on the HG-damaged HUVECs even at the low concentration of eucalyptol (0.04 μg/mL). However, free eucalyptol exerted slight protective effect without statistical differences (**Figure 2B**). Blank carriers LN and CMC/LN showed

almost no protective effect at the corresponding concentration of SPC with the eucalyptol preparations. Moreover, a little exacerbation of the damage was detected in LN group at the highest concentration, which might be closely related to the positive surface potential of LN (**Figure 2C**). It is reasonable to suggest that LN promotes the cellular uptake of eucalyptol and improve the stability of eucalyptol during incubation, which contributes to the remarkable protection effects of ELN. Although CMC/ELN showed inferior cellular uptake to ELN, it exerted similar protective effect on the HG-damaged HUVECs with ELN, which might be attributed to the gradual separation between CMC and ELN and partial protective effect of CMC. In corresponding to the inhibitory effect of LN on the cell viability at the highest concentration of SPC, the protective effect of ELN and CMC/ELN sharply reduced at the highest concentration group. It is proposed that CMC-coating might prevent the positive surface of nanoparticles from interacting with cell membrane within certain limits of lipid concentration. High concentration of LN and ELN with positive surface charge might enhance the contact with HUVECs and compromise the protection effects.

3.5 Antioxidant effect of eucalyptol via regulation on Nrf2 pathway

It is well known that HG-induced vascular endothelium injury is closely related to apoptosis resulted from the intracellular ROS accumulation, leading to the blood pathophysiological change (Rocha Caldas et al., 2015). It is conceivable that eucalyptol maintained the cell viability of HUVECs at the presence of high level of glucose as antioxidant against ROS generation. To evaluate the level of intracellular ROS, a cell-permeable fluorescent marker DCFH-DA was used, which showed fluorescence after oxidation by ROS (**Figure 3**). Compared with the control group, HG incubation significantly increased the ROS level in HUVECs. However, co-incubation with free eucalyptol, ELN and CMC/ELN for 24 h reduced the ROS generation to some extent. In agreement with the results of cell viability, free eucalyptol exhibited slight inhibition effect without statistical significance, while ELN and CMC/ELN exerted obvious antioxidant effect at an equivalent concentration of 1.1 μg/mL eucalyptol, especially for the ELN. It is proposed that effective intracellular delivery of eucalyptol by ELN contributes to the optimum antioxidize

effect. The conflict between interior inhibitory effect on ROS generation and superior cell protection effects of CMC/ELN compared with ELN indicated the crucial role of CMC in the alteration of ELN surface charge leading to more effective cell protection. This data confirmed the necessity of CMC/LN in the promotion of intracellular delivery of eucalyptol as a ROS scavenger.

The underlying mechanisms of the antioxidation effect was further investigated. ROS reduction might be realized through activation of antioxidant and cytoprotective enzymes. The transcription regulator Nrf2 plays a crucial role in the regulation of the endogenous antioxidant system, which combined with its endogenous inhibitor Keap1 before nuclear translocation. As shown in **Figure 4A and B,** exposure of HUVECs to HG reduced the expression of Nrf2 (0.56-fold) and meanwhile increased the protein level of Keap1 (1.14-fold). The free eucalyptol, ELN and CMC/ELN significantly upregulated the expression of Nrf2 and downregulated the level of Keap1 when compared to the HG group, suggesting the transcription factor mediated antioxidant effect of eucalyptol. It was reported that eucalyptol possessed strong affinity to Keap1 and combined at the domain of Nrf2-Keap1 binding site, which activated Nrf2 expression and translocation from cytoplasm to nucleus (Jiang et al., 2019b). Although the expression of Keap1 was decreased after treatment by eucalyptol preparations with statistical difference, slight reduction on the absolute value was detected compared with HG group, indicating that the binding of eucalyptol to Keap1 exerted weak regulation on the expression of Keap1. HO-1 as an essential antioxidant enzyme was significantly reduced to 0.87-fold in HUVECs after exposure to HG (**Figure 4C**), which was in line with reduced expression of Nrf2. The eucalyptol preparations upregulated the expression of HO-1, despite no statistic difference was detected in free eucalyptol group. This data clearly demonstrates that eucalyptol plays the role of ROS scavenger via the Nrf2 pathway. Furthermore, ELN and CMC/ELN exhibited more impressive regulatory effects on the expression of Nrf2, Keap1 and HO-1 than free eucalyptol that might resulted from the improved stability and cellular uptake of eucalyptol.

3.6 In vivo absorption promotion of NR by ELNs

Absorption of ELN and CMC/ELN via oral administration was evaluated by the encapsulated fluorescein-NR. Both NELN and CMC/NELN showed high LR of NR without interference on the drug loading of eucalyptol (**Table S1**). The ELNs altered the plasma concentration time curves of NR (**Figure S3**). After oral administration, ELNs exerted conspicuously increased C_{max} of NR at 30 min, which was the same T_{max} with free NR. The absorption promotion of eucalyptol by vehicles was reflected in the circulation amount of NR. The fast elimination of NR from CMC/NELN and NELN indicating the release of eucalyptol in the circulation that might be contributed to the dissociation of CMC with ELN and disruption of ELN. Moreover, the major pharmacokinetics parameters presented significant increase on the area under the concentration–time curve (AUC) and decrease on plasma clearance (CL) of NR in NELN and CMC/NELN group compared with free NR (**Table S2**). It indicated the prolonged circulation time and improved bioavailability of NR after encapsulation, which further confirmed the absorption promotion effects of ELNs, especially with CMC-coating. Given that sufficient endocytosis of eucalyptol by endothelial cells is the pre-requisite for the pharmacological action, the promoted absorption and prolonged circulation duration of eucalyptol with the help of CMC/LN lays the foundation for the enhanced amelioration effects on HG-damaged vascular endothelial cells.

3.7 Amelioration of endothelial injury in T_1DM rat after eucalyptol formulations treatment

T_1DM rat model was established and orally administrated with eucalyptol preparations according to the schedule in **Figure 5A**. The FBG that was higher than 25 mM at 7^{th} day confirmed the successful establishment of T_1DM rat model (**Figure 5B**). After one-month treatment, the FBG level was merely changed in the T_1DM and eucalyptol groups, while one third of rats in ELN group and half of rats in CMC/ELN group showed low FBG level that was similar with control group (**Figure 5C**). In terms of body weight, eucalyptol preparations treatment reversed the loss of body weight of T_1DM rats (**Figure 5D**). However, the attenuating of T_1DM-related symptoms by eucalyptol preparations was not clear. It was supposed to be closely

related with the protection effects of eucalyptol on hyperglycemia-induced vascular endothelial injury. Histology analysis of thoracic aorta of rats showed the endothelial injury on vascular endothelium in the T_1DM rats induced by hyperglycemia. Compared with the control group, disorganized elastic fibers in aortic tunica media, bulged and degenerated tunica intima and obvious surface lesion was observed in T_1DM group. After one-month treatment by eucalyptol preparations, less tunica intima surface lesion and repaired elastic fibers in tunica media was shown (**Figure 5E**). It is supposed that the hyperglycemia-induced endothelial injury was remarkably ameliorated by the treatment of eucalyptol preparations, especially in CMC/ELN group.

The protective effect of eucalyptol preparations on the T_1DM rats was further verified to be mediated through regulation on Nrf2 pathway via immunofluorescent staining (**Figure 6**) and western blotting (**Figure 7**). In corresponding to the *in vitro* study, T_1DM group exhibited reduced expression on Nrf2 and HO-1 and increased protein level of Keap1, which indicated by the mostly green color in the merged figure. Whereas, the treatment of eucalyptol preparations reversed the tendency on the protein expressions related with the hyperglycemia-induced oxidative stress at different degrees. Eucalyptol and ELN group showed the concurrence of purple grey and orange color, which was the overlap of Nrf2, Keap1 and HO-1 simultaneously. CMC/ELN group showed purple red and orange red color, which indicated the overlap of mostly Nrf2 and HO-1 with less Keap1 (**Figure 6A**). A subsequent statistical analysis on the relative fluorescence intensity of Nrf2, Keap1 and HO-1 made it clearer for the variation of protein expression in each group (**Figure 6B**). The alteration on the protein expression was further confirmed by the western blotting that eucalyptol preparations enhanced the expression of Nrf2 and HO-1, and downregulated the expression of Keap1, especially in CMC/ELN group (**Figure 7**). It was noteworthy that ELN exhibited similar effects with CMC/ELN on the regulation of protein expressions *in vitro*, but obviously inferior effects *in vivo*. It indicated the paradoxical effect of CMC that it impedes the cellular uptake of ELN *in vitro* (**Figure 2**), but partially protects the eucalyptol form the complex gastrointestinal environment

(**Figure 1F**) and promotes the absorption and circulation duration (**Figure S3**). Gradually disassociation between CMC with ELN in the circulation might facilitate the cellular uptake of eucalyptol by endothelial cells. In addition, the inflammatory cytokines including IL-6, IL-1β and TNF-α in the blood was detected at the 37^{th} day (**Figure S2**). However, no obvious inflammatory response was detected in the T_1DM rats, except for IL-1β. As eucalyptol was reported to attenuate the inflammation via suppressing the cytokine secretion (Jiang et al., 2019b), the eucalyptol preparations restored the inflammatory cytokines to the normal level in spite of no statistical difference among free eucalyptol, ELN and CMC/ELN groups. In a word, the protection effects of eucalyptol on hyperglycemia-induced vascular endothelial injury was remarkably improved by the CMC-coated LN in the treatment of T_1DM rats.

4. Conclusion

In this study, we developed a CMC-coated carrier for oral delivery of eucalyptol, which promoted the absorption and prolonged the circulation duration. CMC/ELN conspicuously improved the protection effects of eucalyptol on hyperglycemia-induced vascular endothelial injury via antioxidation effect through regulating on the Nrf2 pathway both *in vitro* and *in vivo*. These results suggested that CMC/ELN can manifested the protection effects of eucalyptol on endothelial injury and may serve as a promising nanoplatform of essential oils for oral administration to increase the therapeutic potential and merits clinical application.

Declaration of competing interest

The authors declare no competing financial interest.

Acknowledgement

This work was financially supported by National Natural Science Foundation of China (No. 81760725 and U1812403-4-4), the Guizhou Provincial Natural Science Foundation (No. [2020]1Z069), the Excellent Young Talents Plan of Guizhou Medical University (No. 2020-102), the Initial Fund for Ph.D. of Guizhou Medical University (No. YJ2018-006), the Fund of High Level Innovation Talents (No. 2015-4029), the Base of International Scientific and Technological Cooperation of Guizhou Province (No. [2017]5802).

References

ABADA, M. B., HAMDI, S. H., GHARIB, R., MESSAOUD, C., FOURMENTIN, S., GREIGE- GERGES, H. & JEM A, J. M. B. 2019. Post- harvest management control of Ectomyelois ceratoniae (Zeller)(Lepidoptera: Pyralidae): new insights through essential oil encapsulation in cyclodextrin. *Pest Manag Sci,* 75**,** 2000-2008.

BILIA, A. R., GUCCIONE, C., ISACCHI, B., RIGHESCHI, C., FIRENZUOLI, F. & BERGONZI, M. C. 2014. Essential oils loaded in nanosystems: a developing strategy for a successful therapeutic approach. *Evid Based Complement Alternat Med,* 2014**,** 651593.

CALDAS, G. F. R., OLIVEIRA, A. R. D. S., ARA JO, A. V., LAFAYETTE, S. S. L., ALBUQUERQUE, G. S., SILVA-NETO, J. D. C., COSTA-SILVA, J. H., FERREIRA, F., COSTA, J. G. M. D. & WANDERLEY, A. G. 2015. Gastroprotective mechanisms of the monoterpene 1,8-cineole (Eucalyptol). *Plos One,* 10**,** e0134558.

DOMINGUETI, C. P., DUSSE, L. M. S. A., CARVALHO, M. D. G. A., DE SOUSA, L. P., GOMES, K. B. & FERNANDES, A. P. 2015. Diabetes mellitus: The linkage between oxidative stress, inflammation, hypercoagulability and vascular complications. *J Diabetes Complications,* 30**,** 738-45.

HAMMOUD, Z., GHARIB, R., FOURMENTIN, S., ELAISSARI, A. & GREIGE-GERGES, H. 2019. New findings on the incorporation of essential oil components into liposomes composed of lipoid S100 and cholesterol. *Int J Pharm,* 561**,** 161-170.

JIANG, F., WU, G., LI, W., YANG, J., YAN, J., WANG, Y., YAO, W., ZHOU, X., HE, Z. & WU, L. 2019a. Preparation and protective effects of 1, 8-cineole-loaded self-microemulsifying drug delivery system on lipopolysaccharide-induced endothelial injury in mice. *Eur J Pharm Sci,* 127**,** 14-23.

JIANG, Z., GUO, X., ZHANG, K., SEKARAN, G., CAO, B., ZHAO, Q., ZHANG, S., KIRBY, G. M. & ZHANG, X. 2019b. The Essential oils and eucalyptol from artemisia Vulgaris L. prevent acetaminophen-induced liver injury by activating Nrf2-Keap1 and enhancing APAP clearance through non-toxic metabolic pathway. *Front Pharmacol,* 10**,** 782.

KIFER, D., MUŽINIĆ, V. & KLARIĆ, M. Š. 2016. Antimicrobial potency of single and combined mupirocin and monoterpenes, thymol, menthol and 1, 8-cineole against Staphylococcus aureus planktonic and biofilm growth. *J Antibiot,* 69**,** 689-696.

KIM, K. Y., LEE, H. S. & SEOL, G. H. 2015. Eucalyptol suppresses matrix metalloproteinase- 9 expression through an extracellular signal- regulated kinase-dependent nuclear factor- kappa B pathway to exert anti- inflammatory effects in an acute lung inflammation model. *J Pharm Pharmacol,* 67**,** 1066-1074.

LIMA, P. R., DE MELO, T. S., CARVALHO, K. M., ARRUDA, B. R., GA, D. C. B., RAO, V. S. & SANTOS, F. A. 2013. 1,8-cineole (eucalyptol) ameliorates cerulein-induced acute pancreatitis via modulation of cytokines, oxidative stress and NF-κB activity in mice. *Life Sci,* 92**,** 1195-1201.

LINGHU, K.-G., WU, G.-P., FU, L.-Y., YANG, H., CHEN, Y., TAO, L. & XIANG-CHUN, S. 2019. 1, 8-Cineole ameliorates LPS-Induced vascular endothelium dysfunction in mice via PPAR-γ dependent regulation of NF-κB. *Front Pharmacol,* 10**,** 178.

LINGHU, K., LIN, D., YANG, H., XU, Y., ZHANG, Y., TAO, L., CHEN, Y. & SHEN, X.

2016. Ameliorating effects of 1, 8-cineole on LPS-induced human umbilical vein endothelial cell injury by suppressing NF-κB signaling in vitro. *Eur J Pharmacol,* 789**,** 195-201.

LIU, J., CHEN, S., BISWAS, S., NAGRANI, N., CHU, Y., CHAKRABARTI, S. & FENG, B. 2020. Glucose- induced oxidative stress and accelerated aging in endothelial cells are mediated by the depletion of mitochondrial SIRTs. *Physiol Rep,* 8**,** e14331.

LOBODA, A., DAMULEWICZ, M., PYZA, E., JOZKOWICZ, A. & DULAK, J. 2016. Role of Nrf2/HO-1 system in development, oxidative stress response and diseases: an evolutionarily conserved mechanism. *Cell Mol Life Sci,* 73**,** 3221-3247.

LOPES, M., SHRESTHA, N., CORREIA, A., SHAHBAZI, M.-A., SARMENTO, B., HIRVONEN, J., VEIGA, F., SEI A, R., RIBEIRO, A. & SANTOS, H. A. 2016. Dual chitosan/albumin-coated alginate/dextran sulfate nanoparticles for enhanced oral delivery of insulin. *J Control Release,* 232**,** 29-41.

MURATA, S., OGAWA, K., MATSUZAKA, T., CHIBA, M., NAKAYAMA, K., IWASAKI, K., KUROKAWA, T., SANO, N., TANOI, T. & OHKOHCHI, N. 2015. 1, 8-Cineole ameliorates steatosis of Pten liver specific KO mice via Akt inactivation. *Int J Mol Sci,* 16**,** 12051-12063.

PYO, Y., TRAN, P., KIM, D. & PARK, J. 2020. Chitosan-coated nanostructured lipid carriers of fenofibrate with enhanced oral bioavailability and efficacy. *Colloids Surf B Biointerfaces,* 196**,** 111331.

ROCHA CALDAS, G. F., OLIVEIRA, A., ARA JO, A. V., LAFAYETTE, S., ALBUQUERQUE, G. S., SILVA-NETO JDA, C., COSTA-SILVA, J. H., FERREIRA, F., COSTA, J. & WANDERLEY, A. G. 2015. Gastroprotective mechanisms of the monoterpene 1, 8-cineole (eucalyptol). *Plos One,* 10**,** 1-17.

SENA, C. M., PEREIRA, A. M. & SEI A, R. 2013. Endothelial dysfunction - A major mediator of diabetic vascular disease. *Biochimi Biophysica Acta,* 1832**,** 2216-2231.

TANG, Y., WU, S., LIN, J., CHENG, L., ZHOU, J., XIE, J., HUANG, K., WANG, X., YU, Y. & CHEN, Z. 2018. Nanoparticles targeted against cryptococcal pneumonia by interactions between chitosan and its peptide ligand. *Nano Lett,* 18**,** 6207-6213.

UPADHYAYA, L., SINGH, J., AGARWAL, V. & TEWARI, R. 2013. Biomedical applications of carboxymethyl chitosans. *Carbohydr Polym,* 91**,** 452-66.

YANG, C., ELEFTHERIADOU, M., KELAINI, S., MORRISON, T., GONZ LEZ, M. V., CAINES, R., EDWARDS, N., YACOUB, A., EDGAR, K. & MOEZ, A. 2020. Targeting QKI-7 in vivo restores endothelial cell function in diabetes. *Nat Commun,* 11**,** 1-17.

YUAN, H., CHEN, J., DU, Y.-Z., HU, F.-Q., ZENG, S. & ZHAO, H.-L. 2007. Studies on oral absorption of stearic acid SLN by a novel fluorometric method. *Colloids Surf B Biointerfaces,* 58**,** 157-164.

List of figures

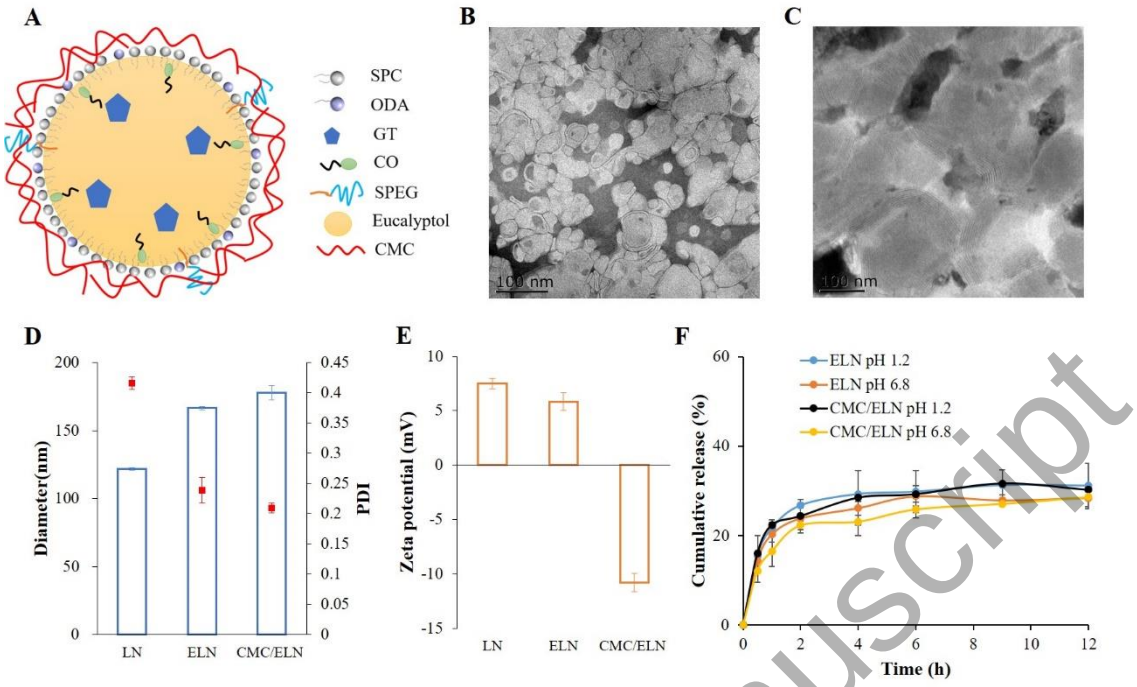

Figure 1. Characteristics of ELN and CMC/ELN. (A) Hypothesized structure of CMC/ELN. Representative TEM images of (B) LN and (C) CMC/ELN (scale bar reads 100 nm). (D) Diameter (bars), PDI (dots) and (E) zeta potential of blank LN, ELN and CMC/ELN. (F) *In vitro* release profiles of eucalyptol from ELN and CMC/ELN at pH 1.2 and 6.8. Each bar represents the mean ± SD (n = 3).

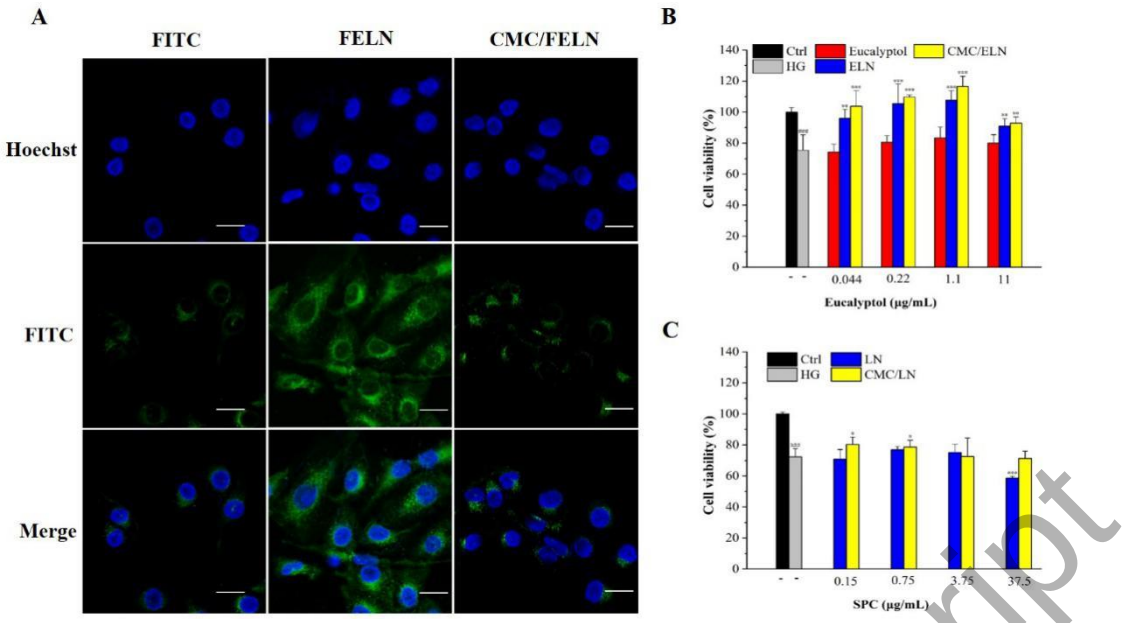

Figure 2. *In vitro* cellular uptake and cytotoxicity. (A) Confocal microscopy images of the intracellular distribution of free FITC, FELN and CMC/FELN in HUVECs after 3 h incubation. Scale bar reads 20 μm. (B) Cytotoxicity on HUVECs treated with free eucalyptol, ELN, CMC/ELN and blank carriers (C) LN and CMC/LN. Each bar represents the means ± SD ($n \geq 5$). Significant difference between Ctrl and HG group is represented as $^{\#\#\#}p < 0.001$. Significant differences from HG group are represented as $^{*}p < 0.05$, $^{**}p < 0.01$, $^{***}p < 0.001$.

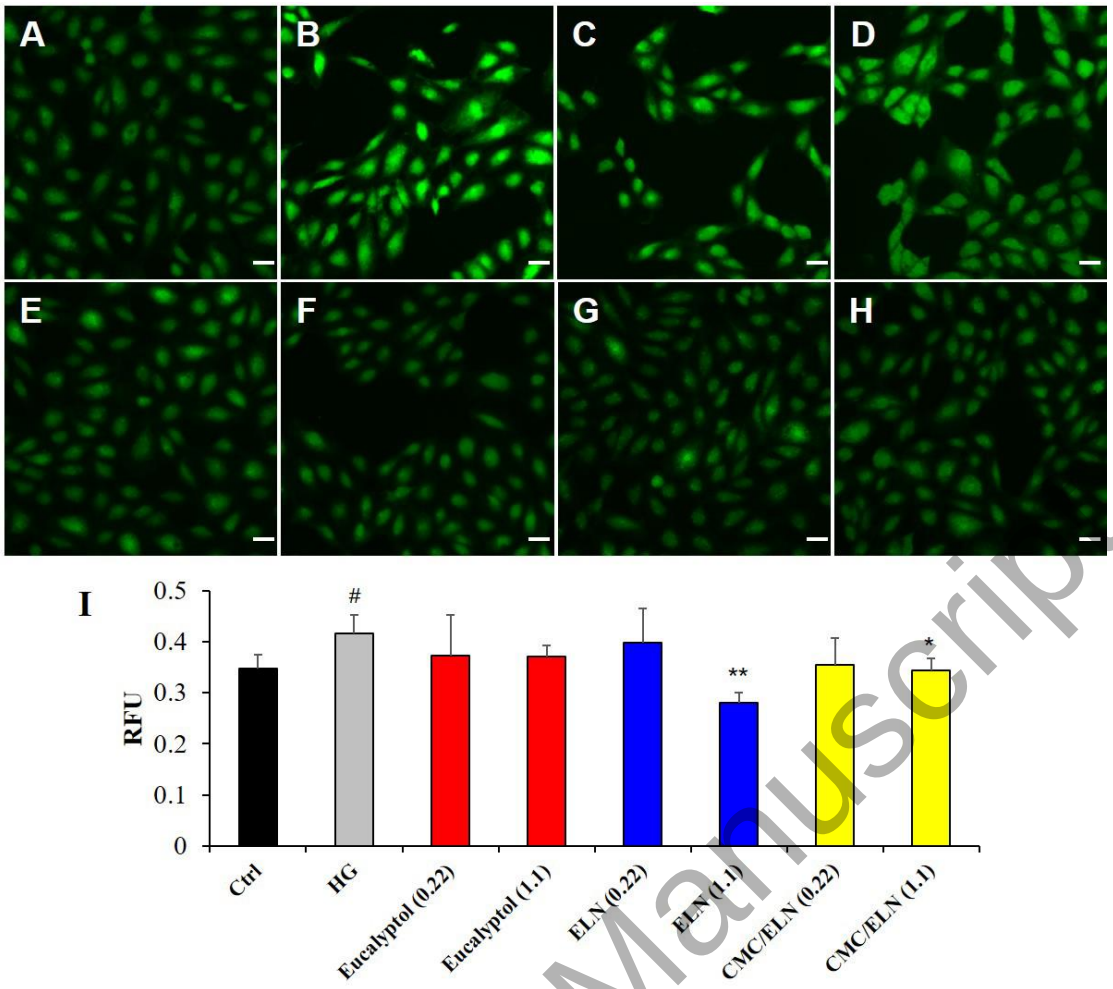

Figure 3. *In vitro* evaluation of intracellular ROS level after treatment for 24 h. The representative view of (A) Ctrl, (B) HG, (C, D) eucalyptol (0.22 and 1.1 μg/mL), (E, F) ELN (0.22 and 1.1 μg/mL), (G, H) CMC/ELN (0.22 and 1.1 μg/mL). Scale bar reads 50 μm. (I) Quantification of the ROS level by the fluorescence intensity. Each bar represents the means ± SD (n = 4). Significant difference between Ctrl and HG group is represented as $^{\#}p < 0.05$. Significant differences from HG group are represented as $^{*}p < 0.05$, $^{**}p < 0.01$.

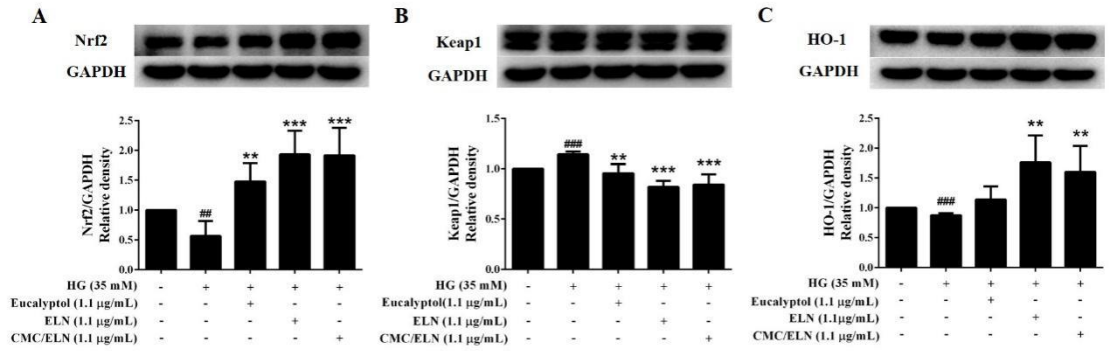

Figure 4. *In vitro* evaluation of protein expression variation of (A) Nrf2, (B) Keap1 and (C) HO-1 after treatment by eucalyptol preparations. Each bar represents the means ± SD (n = 3). Significant difference between Ctrl and HG group is represented as $^{\#\#}p < 0.01$, $^{\#\#\#}p < 0.001$. Significant differences from HG group are represented as $^{**}p < 0.01$, $^{***}p < 0.001$.

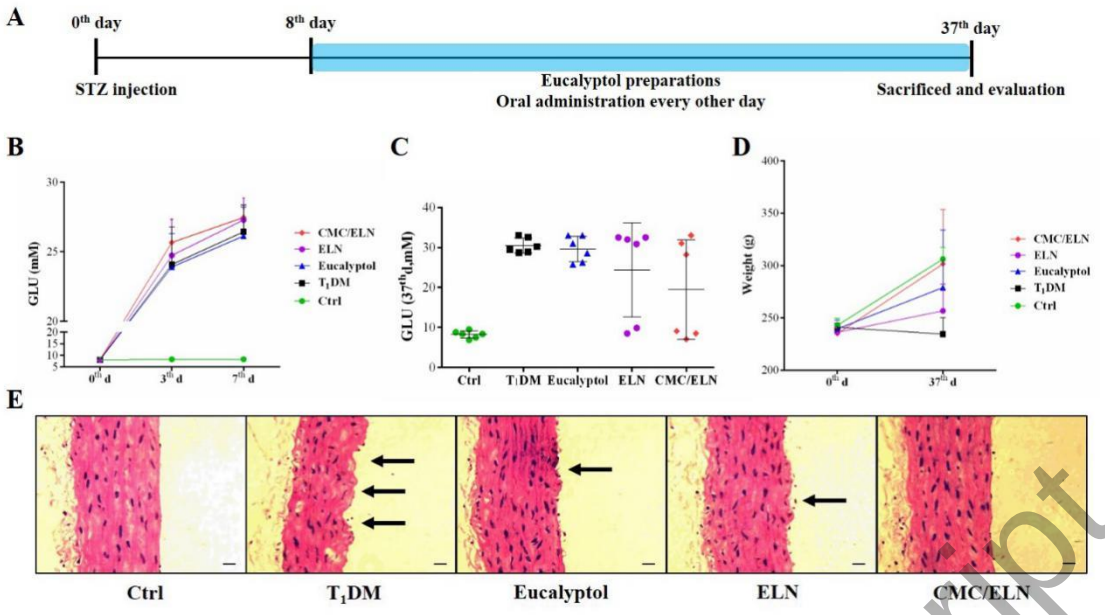

Figure 5. *In vivo* treatment by eucalyptol preparations on T_1DM rats. (A) Schematic illustration of T_1DM rat model establishment and treatments schedule. (B) Blood sugar monitoring within first one week to confirm the establishment of T_1DM rat model. (C) Blood sugar monitoring at the end of experiment. (D) Body weight of rats at the beginning and the end of experiments. (E) Morphology and histologic analysis of thoracic aorta tissues of rats via H&E stain (×100). Black arrows indicate the bulged and degenerated tunica intima and surface lesion. Scale bar reads 75 μm. Each symbol represents the means ± SD (n = 6).

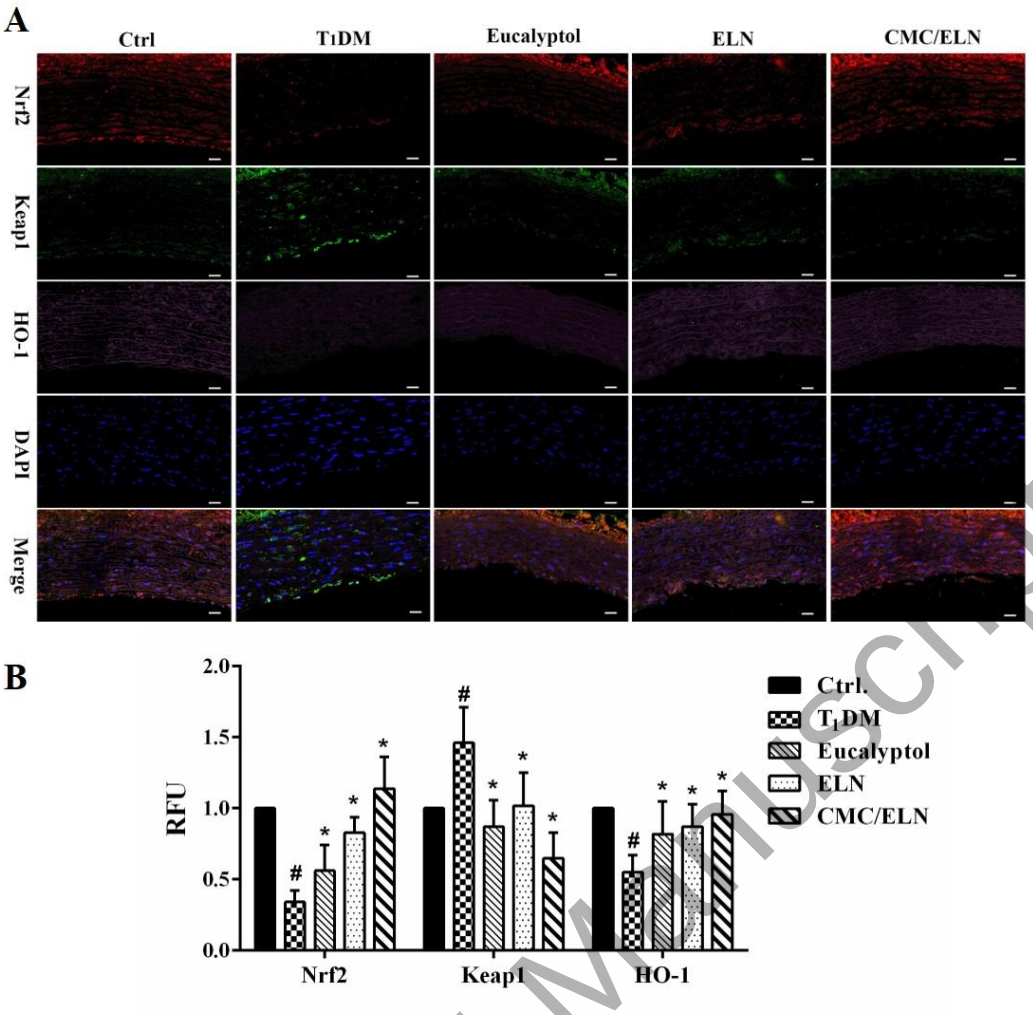

Figure 6. *In vivo* evaluation of protein expression variation of Nrf2, Keap1 and HO-1 after treatment by eucalyptol preparations. (A) The representative view of thoracic aorta tissues in each group via immunofluorescence analysis (×100). Scale bar reads 75 μm. (B) Quantification of the fluorescence intensity of proteins. Each bar represents the means ± SD (n = 3). Significant difference between Ctrl and T_1DM group is represented as $^{\#}p < 0.05$. Significant differences from T_1DM group are represented as $^{*}p < 0.05$.

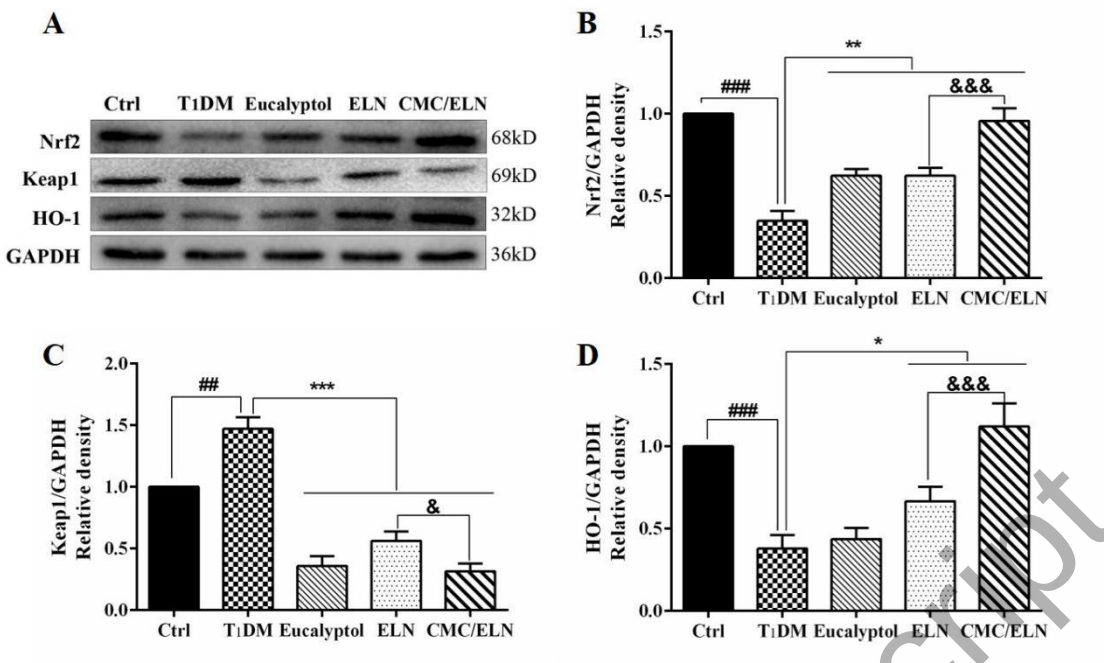

Figure 7. *In vivo* western blotting evaluation of protein expression variation of (A) Nrf2, (B) Keap1 and (C) HO-1 after treatment by eucalyptol preparations. Each bar represents the means ± SD (n = 3, each sample from a different rat). Significant difference between Ctrl and T_1DM group is represented as $^{\#\#}p < 0.01$, $^{\#\#\#}p < 0.001$. Significant differences from T_1DM group are represented as $^{*}p < 0.05$, $^{**}p < 0.01$, $^{***}p < 0.001$. Significant differences from CMC/ELN group are represented as $^{\&}p < 0.05$, $^{\&\&\&}p < 0.001$.

Table 1 Properties of LN and eucalyptol-loaded LNs

Samples	Eucalyptol		Characteristics		
	LC (%)	LR (%)	Diameter(nm)	PDI	Zeta potential (mV)
LN	-	-	121.77 ± 1.10	0.416 ± 0.010	7.51 ± 0.50
ELN	16.19 ± 1.22	77.42 ± 6.86	166.43 ± 1.44	0.239 ± 0.021	5.83 ± 0.80
CMC/ELN	14.81 ± 0.69	73.10 ± 4.04	177.77 ± 5.09	0.209 ± 0.008	-10.77 ± 0.84

Each data represents the mean ± SD of at least three experiments.